

MODELING THE PERFORMANCE OF ULTRAVIOLET REACTOR IN EULERIAN AND LAGRANGIAN FRAMEWORKS

Angelo Sozzi and Fariborz Taghipour*

Chemical and Biological Engineering Department, University of British Columbia, Vancouver, B.C., V6T 1Z3, Canada

ABSTRACT

CFD models for simulating the performance of ultraviolet (UV) reactors for micro-organism inactivation were developed in Eulerian and Lagrangian frameworks, taking into account hydrodynamics, kinetics, and radiation field within UV reactor. In the Lagrangian framework, micro-organisms were treated as discrete particles where the trajectory was predicted by integrating the force balance on the particle. In the Eulerian framework, the conservation equation of species (microorganisms) was solved along with the transport equations. The fluid flow was characterized experimentally using particle image velocimetry (PIV) flow visualization techniques and modeled using CFD for a UV reactor prototype model. The performance of annular UV reactors with an inlet parallel and perpendicular to the reactor axis were investigated. The results indicated that the fluid flow distribution within the reactor volume can significantly affect the reactor performance. Both the Eulerian and Lagrangian models were used to obtain complimentary information on the reactors; while the Lagrangian method provided an estimation of the UV-fluence distribution and the trajectory of species, the Eulerian approach showed the concentration distribution and local photo-reaction rates. The combined information can be used to predict and monitor reactor performance and to improve the reactor design.

NOMENCLATURE

C	Concentration, [mol/L]
D_i	Dose, [mJ/cm ²]
D	Diameter, [cm]
E	Fluence rate, [mW/cm ²]
k	Inactivation rate constant, [cm ² /mJ]
l_i	Distance from lamp point to current point, [cm]
L	Length, [cm]
N	Organism concentration, [PFU/mL]
N_0	Initial organism concentration, [PFU/mL]
n	Number of point sources (MPSS model), [-]
P	Germicidal lamp output per cm, [W/cm]
R	Degradation rate
r	Radial distance from lamp, [cm]
r_l	Radius of lamp sleeve, [cm]
T	Transmissivity of the fluid, [cm ⁻¹]
t	Time, [s]
z	Axial distance on lamp, [cm]
α_i	Fraction of particles receiving dose D_i
σ_w	Absorption coefficient of fluid, [cm ⁻¹]

INTRODUCTION

Ultraviolet –UV– based technologies for water treatment have seen a rapid growth in the past decade due to their potential for micro-organism inactivation and micro-pollutant degradation. UV is capable of inactivating a wide range of bacteria, viruses, and protozoa in aqueous systems. The effect of UV on micro-organisms is due to the photochemical reaction initiated through the absorption of a photon by a molecular structure. This absorption of energy results in photochemical damage to nucleic acids and inactivation of micro-organisms. UV radiation can also result in the destruction of many organic contaminants by photolysis (direct absorption of UV) or photo-initiated oxidation (activation of strong oxidants such as hydrogen peroxide or ozone by UV to form oxidative hydroxyl radicals).

A successful fundamental simulation of UV reactors is the basis for several applications including virtual prototyping, which can lead to cost effective design optimization and performance evaluation. One of the challenges in modeling reactors with spatially dependent reaction rates is the impact of the fluid flow field on the reactor performance. The influence of hydrodynamics on the performance of UV reactors has been widely acknowledged [e.g. Lawryshyn and Cairns, 2003] underlining the importance of detailed flow field information for the design and optimization of UV reactors. Analyzing the performance of photo-reactors therefore involves the integration of a hydrodynamic model, a radiation emission/distribution model, and a kinetic model linked by material and energy balances. The rate of reactions in the kinetic model is linked to the non-homogeneous UV-fluence rate through the local volumetric rate of energy absorption.

Computational Fluid Dynamics (CFD) has been applied to the simulation of hydrodynamics in UV reactors (e.g. Kamimura et al., 2002). Since the accuracy of CFD simulations is dependent on choices made during the model setup, experimental validation of the modeling results by measuring flow characteristics is essential for the effective use of CFD models.

Particle Image Velocimetry (PIV) is a powerful visualization technique to obtain fluid velocities. The general principle of PIV is to illuminate tracer particles in the flow field of interest with a sheet of laser light and acquire two images of the flow field with a known time

separation. The velocity field is determined from the distance traveled by the tracer particles between the two images, divided by the known time interval.

In this work, an integrated CFD-based model was implemented to evaluate the performance of UV reactors. UV-radiation models and volumetric reaction rate models were coupled with reactor hydrodynamics using a commercial CFD code, Fluent 6.2. Annular UV reactors with a concentric lamp parallel to the reactor axis, representing a widely used design for UV reactors, were investigated. The Eulerian and Lagrangian approaches to reactor performance modeling were implemented, combining a spatial UV-fluence rate model with first order kinetics for microorganism inactivation. The reactor performance efficiency (log reduction of UV-reactant material) for a commercially available annular UV reactor was simulated and compared with the biosimetry results. The performance of two reactor geometries, inlet normal to the reactor axis (U-shape) and inlet parallel to the reactor axis (L-shape), were then compared.

MODEL DESCRIPTION

Modelling Flow, Kinetics, and Radiation

Two annular reactor geometries (L=0.89 m, D=0.089 m) with different inlet positions (L- and U-shape) were used in this study (Figure 1). The reactors contained an annular UV lamp (lamp arc L=0.8 m D=0.02 m) and inlet/outlet ports located 3.8 cm from either end for the U-shape, or with the inlet concentric on the front-plate for the L-shape reactor. The reactor flow rate was set at 6.9×10^{-4} m³/s, which corresponds to a mean axial velocity of about 0.11 m/s in the annulus. The following describes the models for reactor hydrodynamics, kinetics, and radiation distribution.

The fluid flow within the UV reactors was simulated through the solution of mass and momentum conservation equations along with the Realizable k-ε turbulence model [Shih et al., 1995] using Fluent CFD software package. Mesh independent solutions were achieved when the computational domain was divided to more than 0.5 million cells. The influence of the Standard k-ε and Realizable k-ε turbulence models on the simulation results was evaluated. The Realizable k-ε model displayed the best overall match to the experimental PIV measurements (see Results and Discussions).

The first order kinetic expression of direct photolysis, in which the degradation rate is a function of the local UV fluence rate, reactant's concentrations, and the reaction rate constant at each point of the reactor, was considered to model the rate of photo-reactant material (e.g. microorganism) degradation.

$$R = \frac{dC}{dt} = -kCE$$

where k is the inactivation rate constant [cm²/mJ], E is the UV-fluence rate [mW/cm²], C is the concentration of photo-reactant material, and t is the exposure time. Micro-organisms can be considered as a photo-reactant material where their concentration is typically expressed by plaque forming units per unit volume, N (similar to C for chemicals). For micro-organism inactivation, based on

the first order kinetics, by integrating the above rate equation the concentration is calculated by:

$$N = N_0 \text{EXP}(-kEt)$$

where N_0 represents the initial organism concentration (plaque forming units per ml) [PFU/ml] and N the organism concentration after UV-exposure [PFU/ml]. MS2 bacteriophage was used as a model micro-organism. An inactivation constant of $k = 0.1$ cm²/mJ has been reported for this microorganism by several sources [e.g. Mulkey, 2003].

The UV irradiance distribution was modeled by the multiple point source summation (MPSS) model [Blatchley, 1997] in which the radiation source (UV lamp) is approximated as a series of point sources emitting diffuse radiation. In this model, the fluence rate (E) at each point is estimated by:

$$E(r, z) = \sum_{i=1}^n \frac{P}{4\pi l_i^2} \exp(-\sigma_w (r - r_i) \frac{l_i}{r})$$

where z and r represent the axial and radial distances, P is the total lamp output, σ_w is the absorption coefficient of the medium, r_i is the lamp sleeve radius, and l_i is the distance from a specific point (r, z) to n_i point source out of a total of n sources.

Modelling Reactor Performance

Reactor performance models were developed in Lagrangian and Eulerian frameworks by integrating the flow, kinetics, and radiation models:

Lagrangian model: In the Lagrangian framework, after obtaining the velocity field by solving the conservation of mass and momentum equations, micro-organisms were treated as discrete particles where the trajectory was predicted by integrating the force balance on the particle. Random effects of turbulence on the particle were accounted for by the discrete random walk model. A statistically significant number of particles (representing microorganisms) were released at the reactor inlet and the absorbed dose was integrated along the path of each particle. The absorbed dose at each point was calculated by multiplying the average local fluence rate (E) by the time period dt that the particle is exposed to that particular local fluence rate. The total dose received by each particle was then calculated by integrating the cumulative dose (fluence) over the path of that particle as:

$$D_i = \int E dt$$

The number of microorganisms that remain vital N_i , out of the N_0 initial number of microorganisms over each dose interval i was calculated by:

$$N_i = \alpha_i \times N_0 \text{EXP}(-kD_i)$$

where α_i is the fraction of particles that receive the dose D_i , k is the inactivation rate constant, and D_i is the average dose for the i th bin interval. The sum of all vital particles over the entire range of doses yields the estimated total number of vital particles (microorganisms) leaving the reactor, N :

$$N = \sum N_i$$

Eulerian model: In the Eulerian framework, the conservation equation of species (microorganisms) was solved along with the transport equations. The local mass

fraction of each species was predicted through the convective-diffusion equation for the species, to calculate the concentration of microorganisms through the domain:

$$\nabla \cdot (\vec{v}C) = -\nabla \cdot \vec{J} + R$$

where J and R are the diffusion flux (including turbulent dispersion) of the species and the source (reaction) rate.

EXPERIMENTS

The flow field was studied experimentally using PIV for mockup UV reactors made of Plexiglas (The details is presented elsewhere [Sozzi and Taghipour, 2005]). PIV measurements were performed using a Flow-map 2D system (Dantec Dynamics) in conjunction with a dual-head Nd:YAG laser (New Wave Research) and a CCD camera (Hamamatsu Photonics) with a resolution of 1344×1024 pixels. The Plexiglas annular reactors ($L=0.89$ m, $D=0.089$ m; inlet/outlet $D=0.019$ m), with a concentric Quartz tube ($D=0.02$ m) were used for the PIV experiments (Figure 1). The water flow rate was set at 6.9×10^{-4} m³/s. The time averaged flow field velocity information from 250 image pairs was considered to assess the accuracy of the CFD modeling results.

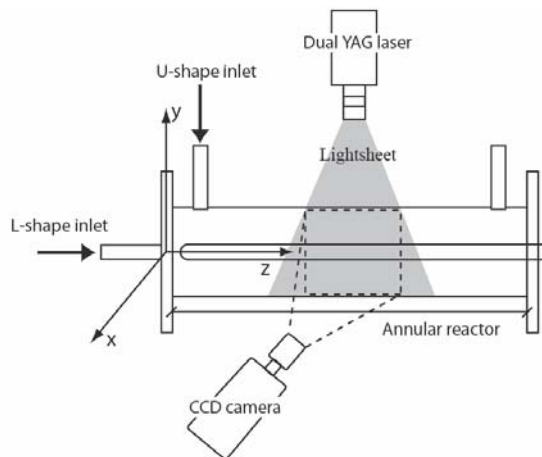


Figure 1: Schematic of the PIV experimental setup. Two UV reactor configurations with inlet perpendicular (U-shape inlet) and parallel (L-shape inlet) to the reactor axis were examined.

RESULTS AND DISCUSSIONS

Evaluation of Reactor Hydrodynamic Model

The flow field in the two UV reactor configurations with an inlet perpendicular (a) and parallel (b) to the reactor axis using time-averaged PIV measurements is shown in Figure 2. The PIV experimental measurements of velocity vectors within the UV reactors are compared with CFD simulations in Figure 3, where vertical lines indicate both positions of the measurements and zero axial velocity. In the reactor with an inlet parallel to the reactor axis, a lamp holder (the three pronged white structure in Figure 2b and light-gray structure in Figure 3b) is required to center and retain the lamp at the entrance of the reactor. In reactor (a), the impinging jet on the central lamp separates and then recombines at the reactor lower wall. The flow at the inlet region of the reactor is non-symmetric with higher velocity at the lower reactor wall. There are also some

regions of flow recirculation (negative velocity) in the upper part of the reactor.

In reactor b, the inlet region exhibits typical expanding jet behavior, including flow recirculation and zones of slow flow close to the reactor inlet. In the region of the lamp holder, the flow deviates from a standard expanding jet pattern. For both reactors, the non-symmetric flow dissipates downstream of the reactor inlet and the flow is distributed nearly evenly in the upper and lower parts of the reactors.

The CFD model was able to predict the relatively complex flow in both U- and L-shape reactors reasonably well and the areas of fast velocity and recirculation flows were predicted by the model (Figure 3). Detailed study of the CFD model parameters indicated that to obtain reliable modeling results of reactor hydrodynamics, enough care need to be taken with the choice of mesh structure and turbulence model [Sozzi and Taghipour, 2006a].

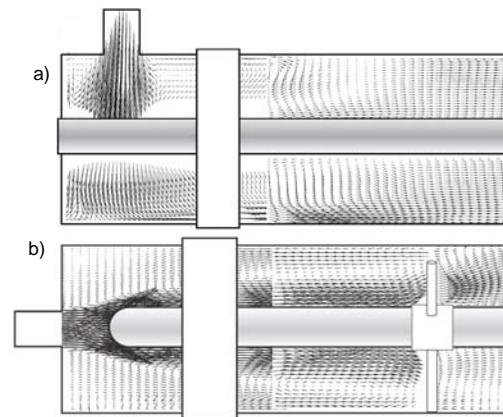


Figure 2: Vectors of velocity magnitude from PIV experimental data at centre planes of UV reactors with an inlet perpendicular, U-shape, (a) and parallel, L-shape, (b) to the reactor axis. The lamp holder is the white structure in Figure b [Sozzi and Taghipour, 2005].

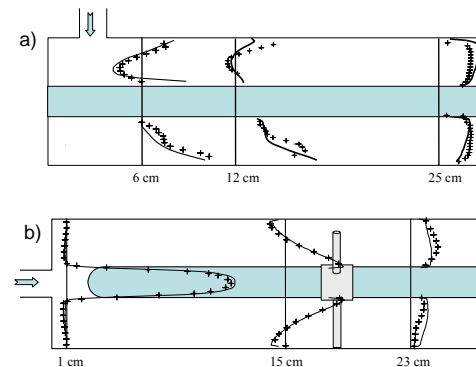


Figure 3: Axial velocity measured by PIV (+) and predicted by CFD (line) in UV reactors with an inlet perpendicular, U-shape, (a) and parallel, L-shape, (b) to the reactor axis. The UV lamps are shown in the centre of the reactors. The lamp holder is the light-gray structure in Figure b. Velocity scales are different for each reactor and various positions [Sozzi and Taghipour, 2006a, 2006b].

Evaluation of Reactor Performance Model

To experimentally evaluate the reactor performance models, a L-shape reactor ($L=0.889$ m, $D=0.089$ m) with similar design to that of a commercial annular UV-disinfection reactor with a UV lamp (lamp power=35 W) containing water with 70% UV-transmittance was simulated applying both the Lagrangian and Eulerian models.

Figure 4 demonstrates the Lagrangian modeling results of particle trajectories calculated by the random walk model, colored by the absorbed dose (fluence). The received dose was calculated by releasing the batches of 500 particles (representing microorganisms) at the reactor inlet. The doses received by the microorganisms were in the range of 21-270 mJ/cm^2 with an average of 68 mJ/cm^2 . The dose distribution calculated by this method corresponds to a log reduction of 1.87 (microorganism inactivation in logarithmic scale).

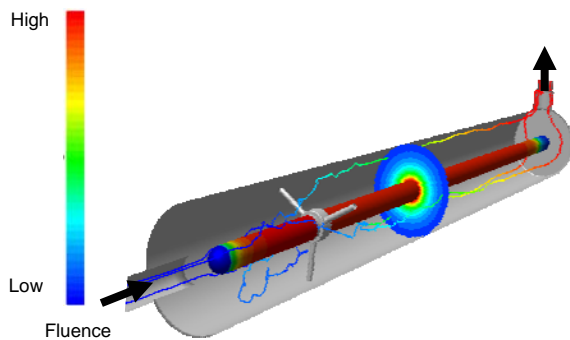


Figure 4: Path of microorganism in a UV reactor colored by UV dose (fluence) [Sozzi, and Taghipour, 2006b]

Figure 5 shows the Eulerian modeling results of the concentration distribution of living microorganisms within the same reactor on a log scale. The effect of the non-uniform fluence rate distribution on the concentration of non-reacted or living microorganisms is clearly visible. The contours of similar concentration are strongly slanted, with lower concentrations close to the lamp surface appearing earlier on the reactor axis. The average mass fractions of microorganisms at both inlet and outlet of the reactor were determined through integration to calculate the reactors total inactivation rate, resulting in a log reduction of 2.07; 10% higher than that predicted by the Lagrangian model.

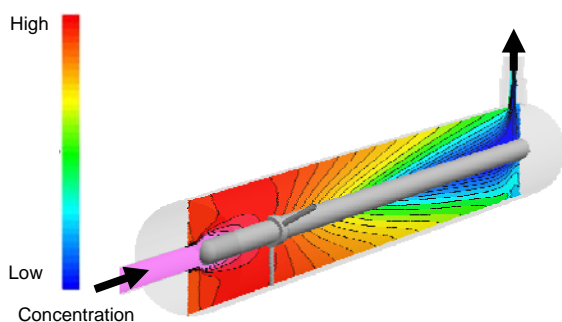


Figure 5: Contours of microorganism concentration (log scale) in a UV reactor [Sozzi, and Taghipour, 2006b]

The deviation between the Eulerian and Lagrangian methods was not examined in depth, but possible causes are the different approaches taken by the two models. The particle trajectories, which are the base of calculation in the Lagrangian method, may not cover the entire domain of UV reactor, causing differences between the results from the two approaches.

The integrated model of UV reactor performance was assessed with experimental data from a commercial UV disinfection reactor with similar design and dimensions [Sozzi and Taghipour, 2006b]. The modeling results for log reduction of micro-organisms using both models were within the experimental measurements (about 1.5 to 2.1 log reduction) of different tests using biosimetry for the commercial UV reactor, indicating the reliability of the integrated reactor performance models.

Modelling Two Reactor Geometries

The performance of two reactor configurations with an inlet perpendicular (U-shape) and parallel (L-shape) to the reactor axis was simulated using the Eulerian method to study the effect of hydrodynamics (as a result of different inlet position) on reactor performance. For both reactors similar dimensions ($L=0.889$ m, $D=0.089$ m), a UV energy output of 35 W for the UV lamp, and a model photo-reactant material with a reaction rate constant of 0.1 (inlet mass fraction of 0.2) were considered.

The overall conversion of the photo-reactant materials (pollutants) in the reactors was calculated by the numerical solutions of the governing equations describing the species transport, species generation/consumption, and the fluence rate within the reactors (Figure 6). The conversion of the photo-reactant material for reactor (a) and (b) was about 3.6 and 4.1 in logarithm scale, respectively. A greater degradation of photo-reactant compounds took place near the UV lamps, where higher radiation fluence rate presents (Figure 6).

Although both reactors comprise the same volume and UV energy available for photo-reaction, the fluid flow in the reactors resulted in the difference in their performance. Reactor (a) has a non-symmetric velocity distribution with higher flow magnitudes in the lower wall of the reactor (Figures 3a). As a result, the degradation of the photo-reactant material in this reactor is non-symmetric, with less mass reduction near the lower reactor wall, because of high flow velocity and low UV fluence rate in these areas (Figure 6-top). Reactor (b), however, provides a different distribution of the flow within the UV reactor, with higher velocity in the areas of high fluence rate (Figures 3b). A symmetric reduction in the mass fraction of the photo-reactant material is observed along the length of this reactor, resulting in a more uniform and higher degradation (Figure 6-bottom). Overall, the concentration profile in reactor (b) is closer to that of a plug-flow reactor, resulting in a higher conversion of photo-reactant material. Reactor (b) is clearly a better design with higher performance for the degradation of micro-organisms. The fact that this performance gain is obtained by a simple change in the inlet placement underlines the importance of

including hydrodynamic considerations into reactor design.

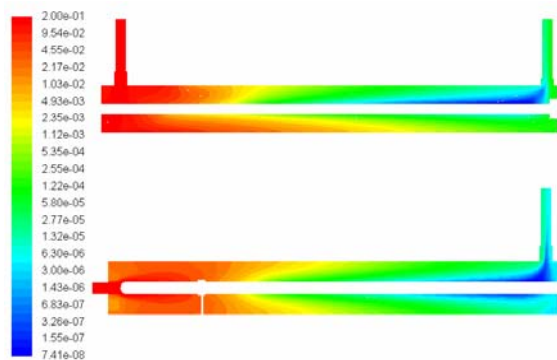


Figure 6: Contours of mass fraction of photo-reactive material in reactors with an inlet perpendicular to the reactor axis (top) and with an inlet parallel to the reactor axis (bottom). The inlet mass fraction of photo-reactant materials was set at 0.2

CONCLUSION

UV reactor performance models based on the Lagrangian and Eulerian methods were successfully implemented in a commercial CFD code and provided results in good agreement with the experimental data. Both models can be used to gain complimentary information on the same reactor; while the Lagrangian method provides estimates of the UV-dose distribution and the particle tracks visualize flows patterns, the Eulerian approach shows the concentration distribution and local reaction rates. The combined information can be used to predict and monitor reactor performance levels and to improve the reactor designs. At a higher computational cost, the Eulerian model delivers a more conclusive image of the local concentration within the reactor volume. More importantly, this model can be extended to accommodate more complicated reaction steps, which is the characteristic of UV oxidation reactors for removing organic contaminants.

Simulation results from the modeling of two conceptual reactor designs indicated that the fluid flow distribution within the photo-reactor volume affects the performance, because of the non-uniform distribution of the fluence rate in the reactors and the dependency of the photo-reaction rate on UV fluence rate.

REFERENCES

- Blatchley, E. R., (1997) "Numerical modeling of UV intensity: Application to Collimated Beam Reactors and Continuous Flow Systems", *Water Res.* 31, 9, 2205-2218
- Kamimura, M., Furukawa, S., Hirotsuji, J. (2002) "Development of a simulator for ozone/UV reactor based on CFD analysis", *Water Sci. Technol.* 46, 13-19

Lawryshyn, Y. A., and Cairns, B. (2003) "UV disinfection of water: the need for UV reactor validation", *Water Science & Technology: Water Supply* 3, 293-300.

Mulkey, L. A. (2003) ETV Joint verification statement, UV disinfection of secondary effluent system by Suntec Inc", *Technical Report*, US-EPA, Environmental Technology Verification Program.

Shih, T. H., Liou, W. W., Shabbir, A., Yang, Z., Zhu, J. (1995) A new k- ϵ eddy viscosity model for high Reynolds number turbulent flows model development and validation. *Computers Fluids* 24, 227-238.

Sozzi, A. and Taghipour, F. (2005) "Experimental Investigation of Flow Field in Annular UV Reactors Using PIV", *Ind. Eng. Chem. Res.*, 44, 9979-9988

Sozzi, A. and Taghipour, F. (2006a) "Computational and Experimental Study of Annular Photo-Reactor Hydrodynamics", *Int. J. Heat Fluid Flow*, accepted January 2006 (Available online March 2006)

Sozzi, A. and Taghipour, F. (2006b) UV Reactor Performance Modeling by Eulerian and Lagrangian Methods, *Environ. Sci. Technol.*, 40, 1609-1615